

Numerical calculation of relative dose rates from cylindrical ^{32}P and ^{90}Y beta sources used in intravascular brachytherapy

E. de Paiva¹

¹*Divisão de Física Médica, Instituto de Radioproteção e Dosimetria – IRD/CNEN/MCTI, 22783-127, Rio de Janeiro – RJ, Brasil*

epaiva@ird.gov.br

(Recebido em 24 de abril de 2014; aceito em 12 de agosto de 2014)

Beta-particle sources can be used in radiotherapy to treat several diseases. In particular cylindrical (seed) beta-minus sources have been used in cardiology for the prevention of restenosis of coronary artery. Two radioisotopes suitable to be used in intravascular brachytherapy treatment of arteries are the pure beta-emitters ^{32}P and ^{90}Y . In this work a routine calculation to estimate absorbed dose rate distributions around cylindrical sources containing the beta emitters ^{32}P and ^{90}Y has been developed in order to handle with various configurations of radii, lengths and distances in a faster and simple way. The results of relative dose rates are compared with published dose distributions for ^{32}P and $^{90}\text{Sr}/^{90}\text{Y}$ sources using the Monte Carlo method and a good agreement (differences < 6 %) has been found in the region of clinical interest measured from the cylindrical source center.

Keywords: Brachytherapy. Beta particles. ^{32}P . ^{90}Y .

Cálculo das taxas de dose relativas de fontes cilíndricas de ^{32}P e ^{90}Y usadas em braquiterapia intravascular.

Fontes de partículas beta podem ser usadas em radioterapia para o tratamento de várias doenças. Em particular fontes beta-menos cilíndricas (sementes) têm sido usadas em cardiologia para a prevenção da restenose das artérias coronárias. Dois radioisótopos adequados para serem utilizados em braquiterapia intravascular no tratamento de artérias são os emissores beta puros ^{32}P e ^{90}Y . Neste trabalho foi desenvolvido uma rotina de cálculo para estimar as distribuições de taxas de dose absorvida em torno de fontes cilíndricas contendo os emissores beta ^{32}P e ^{90}Y de modo a lidar com várias configurações de raios, comprimentos e distâncias de forma rápida e simples. Os resultados de taxas de dose relativas são comparados com as distribuições de dose publicadas para as fontes ^{32}P e $^{90}\text{Sr}/^{90}\text{Y}$ obtidas usando o método Monte Carlo e um bom acordo (diferenças < 6%) foi encontrado na região de interesse clínico medido a partir do centro da fonte.

Keywords: Braquiterapia. Partículas beta. ^{32}P . ^{90}Y .

1. INTRODUCTION

Low energy photon sources, due to the low penetration photons, and beta particle emitting sources, due to the short range of electrons in tissue, and consequent rapid decrease of dose with distance, are widely used in brachytherapy for the treatment of several diseases. Several radionuclides can be used or have the potential to be used in brachytherapy, such as ^{198}Au , $^{188}\text{W}/^{188}\text{Re}$, ^{188}Re , ^{186}Re , ^{181}W , ^{169}Yb , ^{145}Sm , $^{144}\text{Ce}/^{144}\text{Pr}$, ^{133}Xe , ^{109}Cd , ^{62}Cu and ^{48}V , but the most commonly used radionuclides in brachytherapy treatments are ^{125}I and ^{103}Pd (low-energy photon sources), and $^{106}\text{Ru}/^{106}\text{Rh}$, $^{90}\text{Sr}/^{90}\text{Y}$, ^{90}Y and ^{32}P (beta-particle sources) [1].

Clinically, low-energy photon and beta-particle sealed sources have been used for the treatment of several diseases. For example, in ophthalmology applicators containing $^{106}\text{Ru}/^{106}\text{Rh}$, plaques of ^{60}Co and seeds of ^{125}I have been used for decades for the treatment of malignant melanoma of the choroid [2-9], and plaques of $^{90}\text{Sr}/^{90}\text{Y}$ have been used for post-operative treatment of pterygia [10] and have also been used for the treatment of retinoblastoma [11].

Others clinical applications include the use of seeds of ^{125}I and ^{103}Pd for permanent implants in the therapy of tumors of the prostate and central nervous system [12-14] and the use of sources containing the beta emitters $^{90}\text{Sr}/^{90}\text{Y}$ and ^{32}P for the treatment of coronary artery diseases [15]. This intravascular brachytherapy assumes a special importance if we take in account the increasing rates of mortality and morbidity due to cardiovascular diseases all over the world [16].

In the particular case of beta-ray sealed sources used in the radiation therapy of coronary artery diseases an accurate dosimetry is needed so as to irradiate the region of interest and the normal tissue be compromised as less as possible [17-20]. Therefore, the success of treatment depends strongly on accurate measurements of the dose distributions. An accurate determination of absorbed dose distributions around the beta source is not an easy task, mainly due to the high-dose gradient and the short range of beta-particles as compared with the size of detectors and, in some cases, the non-uniform distribution of radioactive material over the source surface can bring additional problems to the measurements. All difficulties encountered in measurements of beta-ray dose distributions do calculation methods increase in importance.

The absorbed dose distributions around beta ray sources used in brachytherapy are basically calculated by two general methods. i) Monte Carlo methods for electron transport [21], and ii) analytical and numerical methods [22-25]. Using Monte Carlo methods, it is possible to deal with more complex and realistic geometries and different media and obtain results with accuracy that can be comparable with measurements, but may be very time-consuming and may not be available for daily use in the medical facility. The analytical and numerical methods are based on the knowledge of beta point-source dose functions and may give results of absorbed dose distributions more rapidly, but may present a little accuracy and apply only for homogeneous medium with uniform density. Following the second approach and using the FORTRAN programming language, which some versions of compiler can be freely downloaded from the web, in this work a routine calculation was developed for numerical integration of a beta point-source dose function around cylindrical sources of ^{32}P and ^{90}Y used in intravascular brachytherapy treatment. The estimates of absorbed dose distributions in water around line sources of ^{32}P and ^{90}Y obtained in this work have been compared with results obtained by Monte Carlo simulations [26-28].

2. MATERIALS AND METHODS

In the fifties Loevinger proposed a simple analytical function describing the dose distribution in tissue around a point source (or point kernel) of a beta-particle emitter [22]. Almost 30 years later Vynckier and Wambersie proposed a slight modification on the Loevinger formula in order to obtain a better fit of function to experimental data [23,24]. The modified function that describes the absorbed dose rate $J(\xi)$ around a beta point source of brachytherapy as a function of the distance ξ from the source can be expressed by

$$J(\xi) = \frac{B}{(\rho v \xi)^2} \left\{ c \left[1 - \frac{\rho v \xi}{c} \exp \left(1 - \frac{\rho v \xi}{c} \right) \right] + \rho v \xi \exp(1 - \rho v \xi) - \rho v \xi \left(1 - \frac{\rho v \xi}{2} - \frac{f}{2} \right) \right\}, \quad (1)$$

where ρ is the density of the medium and v is the absorption coefficient, with

$$\left[1 - \frac{\rho v \xi}{c} \exp \left(1 - \frac{\rho v \xi}{c} \right) \right] \equiv 0, \quad (2)$$

for $\rho v \xi \geq c$, and

$$J(\xi) \equiv 0, \quad (3)$$

for $\rho v \xi \geq f$.

The parameter B is a normalization constant given by

$$B = 0.046 \rho^2 v^3 \overline{E_\beta} \alpha \quad (4)$$

where $\overline{E_\beta}$ is the mean kinetic energy of the beta particle, and the constant α depends on the dimensionless parameters c and f (introduced in references [22-24] to improve the fit of function

$J(\xi)$ to available experimental and theoretical data. In this work updated values obtained by Monte Carlo method is used, as described in reference [1]) as

$$\frac{1}{\alpha} = 3c^2 - (c^2 - 1) \exp(1) + (3 + f) \exp(1 - f) - 4 \exp\left(1 - \frac{f}{2}\right). \quad (5)$$

In the case of extended beta rays sources Equation (1) must be integrated over the surface or the volume of the source so as to obtain the dose rates at a given point. In the use of Equation (1) the following assumptions are adopted. The medium is homogeneous with density ρ ; the radioactive material is uniformly distributed on the surface or over the volume of the source; the source and absorber medium have the same composition and density, and the encapsulation of radioactive material is not considered.

The sources analysed in this work were single line (seed) sources containing the pure beta-minus emitters ^{32}P and ^{90}Y , chosen because of its importance in intravascular brachytherapy [16]. The ^{32}P (produced by irradiation of ^{32}S with moderately fast neutrons) and ^{90}Y (produced by neutron activation of ^{89}Y) sources have half-lives respectively equal to 14.26 and 2.67 days and maximum beta energy respectively equal to 1.71 and 2.28 MeV. Both sources are cylinders of radius a and height L , and because of symmetry a cylindrical system of coordinates was chosen with its origin located at the center of the cylinder, as shown in Figure 1. For line sources with radius < 0.05 cm is recommended that the position $(y, z) = (y_0, z_0) = (0.20 \text{ cm}, 0 \text{ cm})$ be taken as the reference point [1].

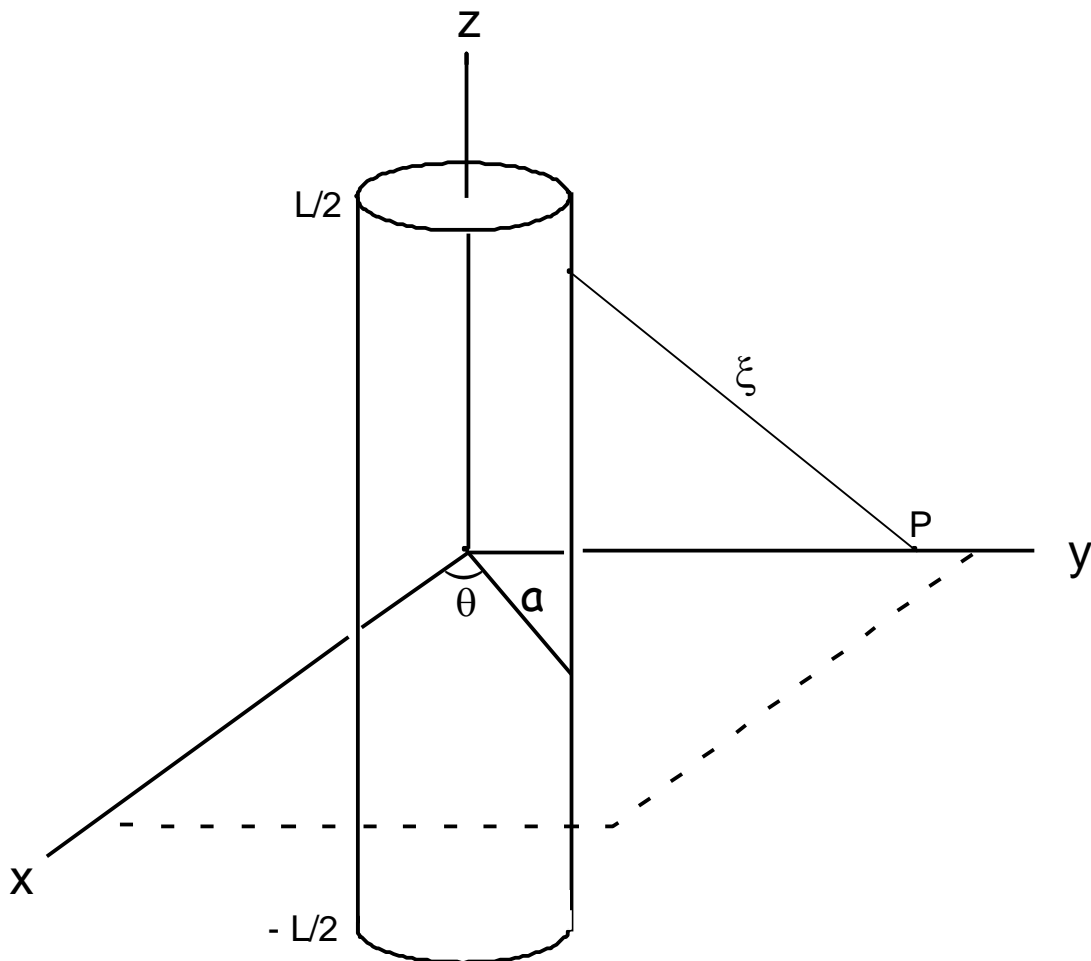


Figure 1. The geometry of a cylindrical beta-ray source of radius a and length L used for integration of the beta point dose function.

The absorbed dose rates \dot{D} at the point P in Figure 1 are obtained by integration of Equation (1) carried out over the surface of each cylindrical source of radius a and length L and can be written as

$$\dot{D} = a_S \int_S J(\xi) \cdot dS, \quad (6)$$

where a_S is the surface activity and dS is the area element, or

$$\dot{D} = a_S \iint_S J(\xi) \cdot a \, d\theta \, dz. \quad (7)$$

Here the radial coordinate is the constant radius a , θ is the azimuthal angle in the xy -plane from the x -axis with $0 \leq \theta \leq 2\pi$, and z is the axial coordinate with $-L/2 \leq z \leq L/2$. For the geometry depicted in Figure 1, variables ξ , θ and z are related by expression

$$\xi^2 = y^2 + a^2 - 2ay \sin \theta + z^2. \quad (8)$$

A simple calculation code written in FORTRAN has been developed for the numerical integration of Equation (7) to evaluate the absorbed dose rates in water from cylindrical ^{32}P and ^{90}Y beta sources used in intravascular brachytherapy for various configurations of radii, lengths and distances. The method of integration was based on trapezoidal rule and the obtained results were validated by making a comparison with the other available different simulations data.

3. RESULTS AND DISCUSSION

In the above equations the medium is considered equivalent to water with a density $\rho = 1 \text{ g/cm}^3$; the absorption coefficient ν is equal to $8.24 \text{ cm}^2/\text{g}$ for ^{32}P source and $5.05 \text{ cm}^2/\text{g}$ for ^{90}Y source; the mean beta energy per disintegration \overline{E}_β is 0.695 MeV for ^{32}P source and 0.933 MeV for ^{90}Y source; the dimensionless parameters c and f are respectively 0.92 and 5.28 for ^{32}P and 0.95 and 4.48 for ^{90}Y . The surface activity a_S is 1 MBq/cm^2 for both sources. The sources considered in this study have radii a ranging from 0.01 to 0.045 cm and lengths L ranging from 0.25 to 3 cm ; the estimates were carried out to radial distances in the interval $0.02 \text{ cm} \leq y \leq 0.9 \text{ cm}$ and axial distances in the interval $0 \text{ cm} \leq z \leq 1.6 \text{ cm}$.

Considering the dimensions of the sources described in Figures 2, 3 and 4, they were chosen in order to match the commercially available intravascular brachytherapy sources ^{32}P (Guidant Corporation, Houston, TX) and $^{90}\text{Sr}/^{90}\text{Y}$ (Novoste Corporation, Norcross, GA) [16].

In part a) of Figure 2, relative absorbed dose rates in water are shown due to ^{32}P line source. They are plotted against the radial distance measured from the z -axis of a 2.0 cm long cylinder with radius of 0.012 cm . The results of this work (solid lines) are relative to the reference point and calculated for $z = 0$ (upper curve) up to $z = 1.6 \text{ cm}$ (lower curve). Results have indicated that up to $z \lesssim 0.6 \text{ cm}$ the dose rates are equal and they are negligible for the region $z > 1.6 \text{ cm}$. For comparison, published relative dose rates obtained by Monte Carlo simulations (squares and triangles) for $z = 0 \text{ cm}$ [26,27] and $z = 1.0 \text{ cm}$ [27] are also shown. A good agreement (differences $< 6 \%$) was found in the region of clinical interest ($y \lesssim 0.5 \text{ cm}$). In part b) of Figure 2, relative absorbed dose rates in water due to ^{90}Y line source are shown. They are plotted against the radial distance measured from the z -axis of a 0.25 cm long cylinder with radius of 0.028 cm . The calculated values of this work (solid lines) are relative to the reference point and calculated for $z = 0$ (upper curve) up to $z = 0.5 \text{ cm}$ (lower curve), with the omission of labels $z = 0.2$ and $z = 0.4 \text{ cm}$. For comparison, published relative dose rates obtained by Monte Carlo simulations (circles) for $^{90}\text{Sr}/^{90}\text{Y}$ beta source for $z = 0 \text{ cm}$, $z = 0.3 \text{ cm}$ and $z = 0.5 \text{ cm}$ [28] are also shown and a fairly agreement (differences $< 5 \%$) was found in the region of $y \lesssim 0.7 \text{ cm}$ and $z = 0 \text{ cm}$. It should be pointed out that such a comparison is only possible because the dose

due to the $^{90}\text{Sr}/^{90}\text{Y}$ beta source are originated mainly due to the daughter isotope ^{90}Y due to its higher energy beta particles emitted. As can be seen from Figure 2 both sources exhibit a general trend of decreasing doses with the increase of z and doses decrease steeply at region beyond of $\xi = f/\rho v$.

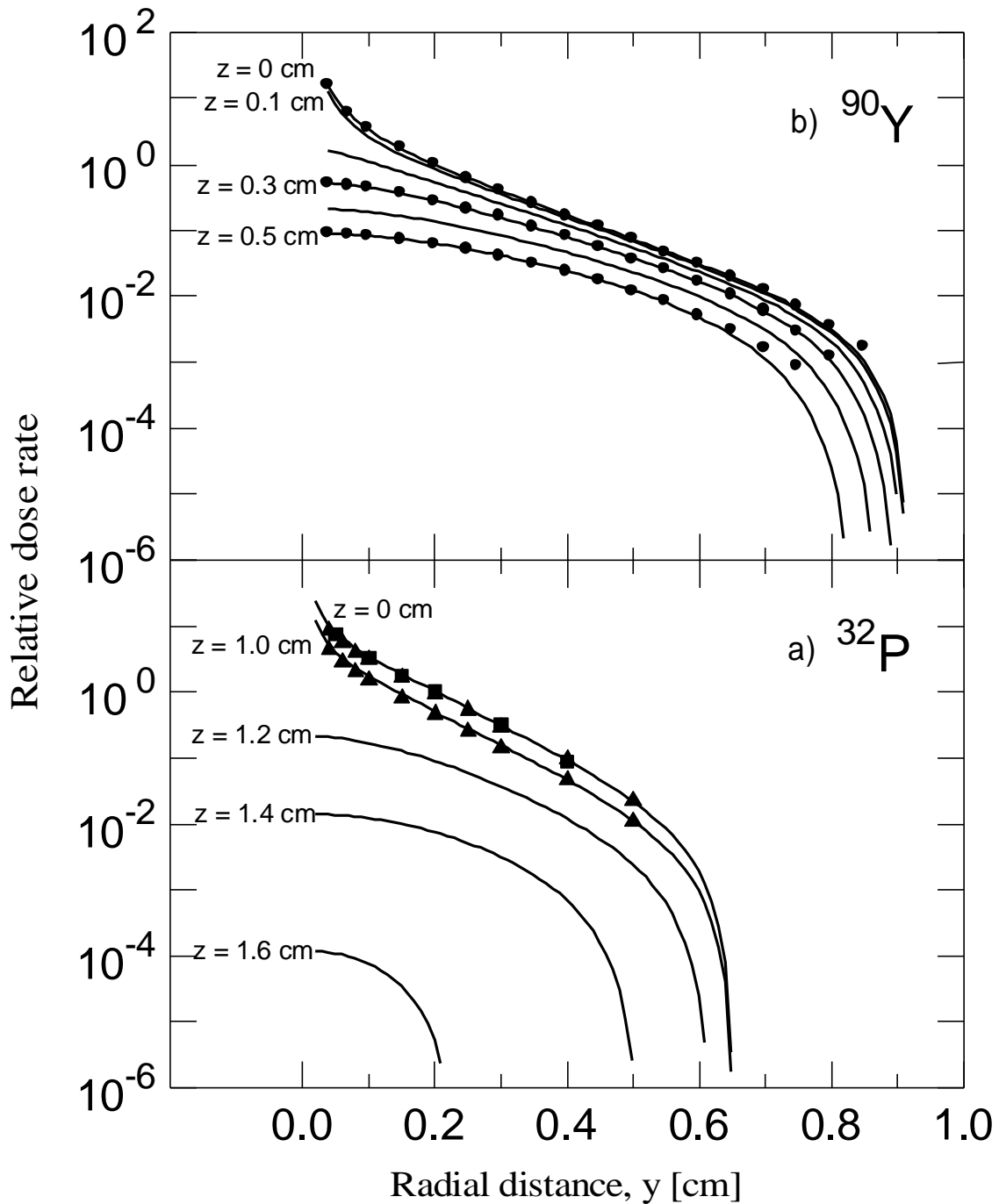


Figure 2. Relative dose rates as a function of the radial distance for a fixed radius $a = 0.012$ cm and length $L = 2.0$ cm (^{32}P source, part a)) and $a = 0.028$ cm and length $L = 0.25$ cm (^{90}Y source, part b)). Dose rates are calculated for various axial positions and are relative to the dose rate at the reference point. Monte Carlo studies for the ^{32}P (squares [26], triangles [27]) and ^{90}Y (circles [28]) sources are presented as well.

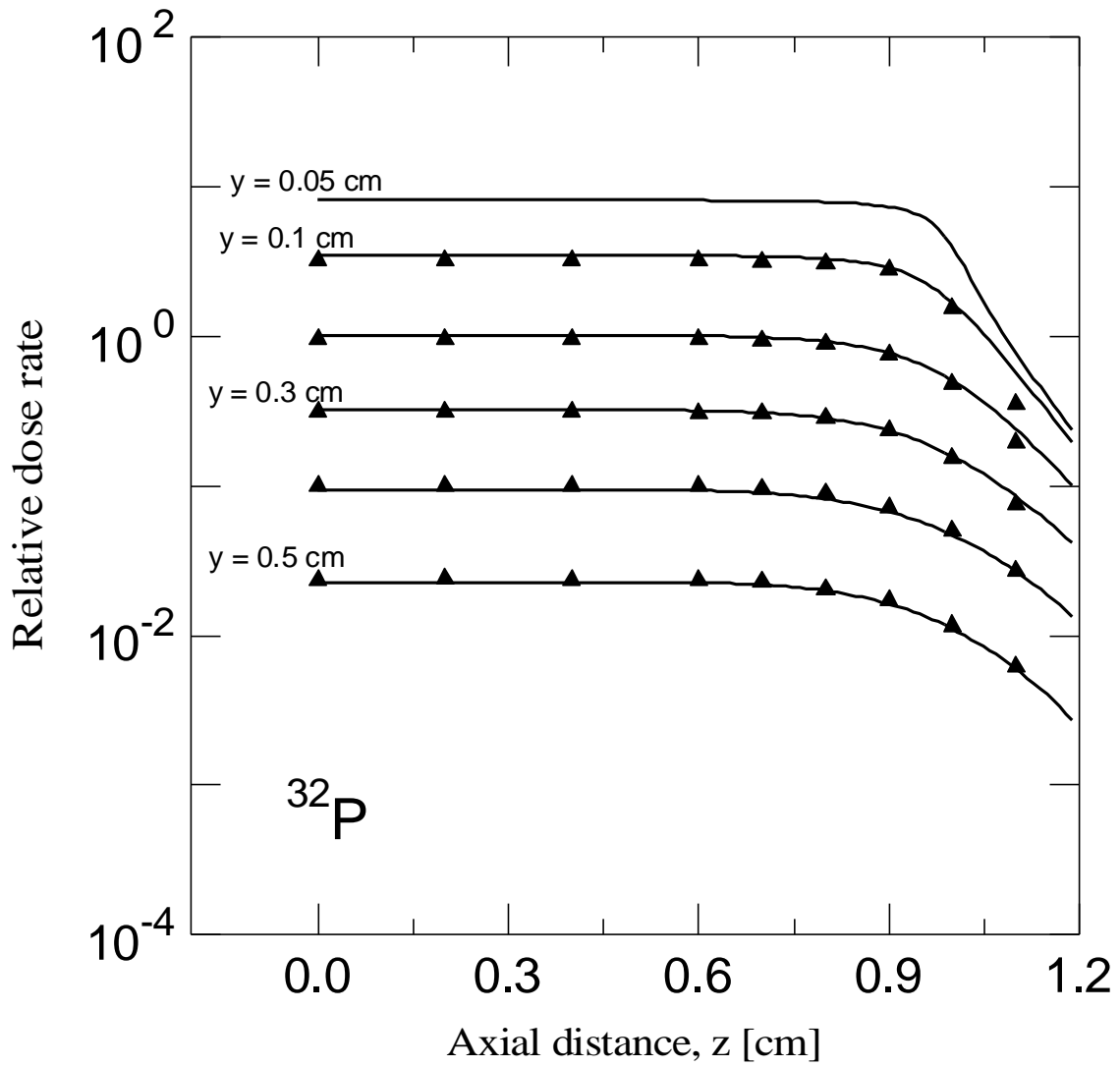


Figure 3. Relative dose rates as a function of the axial distance for a ^{32}P beta source with radius $a = 0.012$ cm and length $L = 2.0$ cm. Dose rates are calculated for various radial positions and are relative to the dose rate at the reference point. The triangles are published results obtained by Monte Carlo simulation [27].

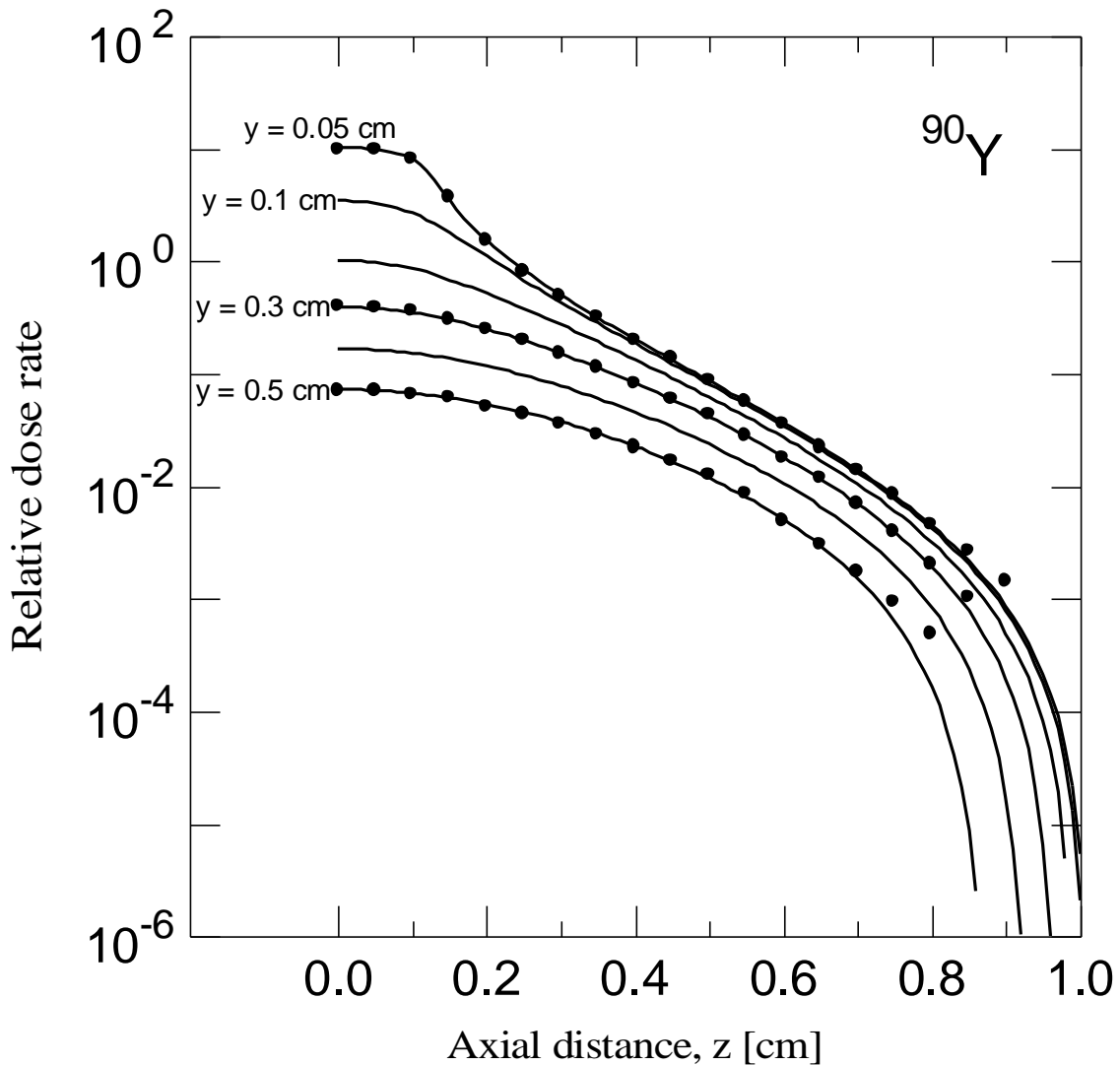


Figure 4. Relative dose rates as a function of the axial distance for a ^{90}Y beta source with radius $a = 0.028$ cm and length $L = 0.25$ cm. Dose rates are calculated for various radial positions and are relative to the dose rate at the reference point. The circles are published results obtained by Monte Carlo simulation [28].

It can also be seen that the relative dose rates start with an exponential decrease near the surface of both sources up to $z \lesssim L/2$ cm. In general a good agreement was found in the entire region, however a disagreement is observed at large radial distances. This discrepancy may be ascribed to the simplified assumptions adopted in the use of the beta-ray point kernel dose function.

In Figure 3 the absorbed dose rates from the ^{32}P source are plotted against the axial distance measured from the centre of a 2.0 cm long cylinder with radius of 0.012 cm. The results (solid lines) are relative to the reference point and calculated for $y = 0.05$ cm (upper curve) up to $y = 0.5$ cm (lower curve), with the omission of labels $y = 0.2$ and $y = 0.4$ cm. As can be seen the source exhibits a general trend of decreasing relative doses with the increase of y . The relative dose rates from the ^{32}P source are constant for z -values up to $\sim L/2$ and near the surface. For comparison, reported results of Monte Carlo simulations of relative dose rates (triangles) for the ^{32}P beta source for $y = 0.1$ cm, $y = 0.2$ cm, $y = 0.3$ cm, $y = 0.4$ cm and $y = 0.5$ cm [27] are also shown. A good agreement (differences $< 6\%$) was found for axial distances up to ~ 1.0 cm.

Figure 4 presents the absorbed dose rates from the ^{90}Y source plotted against the axial distance measured from the centre of a 0.25 cm long cylinder with radius of 0.028 cm. Results (solid lines) are relative to the reference point and calculated for $y = 0.05$ cm (upper curve) up to $y = 0.5$ cm (lower curve), with the omission of labels $y = 0.2$ and $y = 0.4$ cm. As can be seen the

source exhibits a general trend of decreasing relative doses with the increase of y . The relative dose rates from the ^{90}Y source are almost constant for the region near the surface and with $z \lesssim L/2$. For comparison, results of Monte Carlo simulations of relative dose rates (circles) for the $^{90}\text{Sr}/^{90}\text{Y}$ beta source for $y = 0.05$ cm, $y = 0.3$ cm and $y = 0.5$ cm [28] are also shown. A good agreement (differences < 10 %) was found for axial distances up to ~ 0.7 cm then a poorer agreement is observed.

Figure 5 shows the absorbed dose rates from cylindrical sources of ^{32}P (part a) and ^{90}Y (part b) plotted against the length of the cylinder for radii ranging from $a = 0.015$ cm to $a = 0.045$ cm. Results are normalised to the source with $L = 2.0$ cm and $a = 0.015$ cm at the reference point in part a), and $L = 0.25$ cm and $a = 0.015$ cm at the reference point in part b). It can be noted that in all cases the dose rates increase quickly at low lengths up to a maximum, determined by the range of beta particles, and then remain constant as length increases from ~ 0.8 cm (^{32}P source) or ~ 1 cm (^{90}Y source) on.

Figure 6 depicts the absorbed dose rates from cylindrical sources of ^{32}P (part a) and ^{90}Y (part b) as a function of the radius of the cylinder for various lengths L . Results are normalised to the source with $L = 2.0$ cm and $a = 0.01$ cm at the reference point in part a), and $L = 0.25$ cm and $a = 0.01$ cm at the reference point in part b). It can be seen that relative dose rates have a linear growth with the radius. From Figure 6 can be clearly seen that the differences between successive dose rates curves diminish as the length increases and are equal to zero for $L \geq 1$ cm (^{32}P source) and $L \geq 1.5$ cm (^{90}Y source).

Despite the good results observed in Figures 2-4, attention should be paid to the limitations of the calculation method, i.e. the surrounding medium is formed by water only and is uniform. This homogeneity is changed by the encapsulation of radioactive material, and scattering of beta particles in this encapsulation material is not taken into account in the integration of point-source dose function and may contribute to some discrepancies.

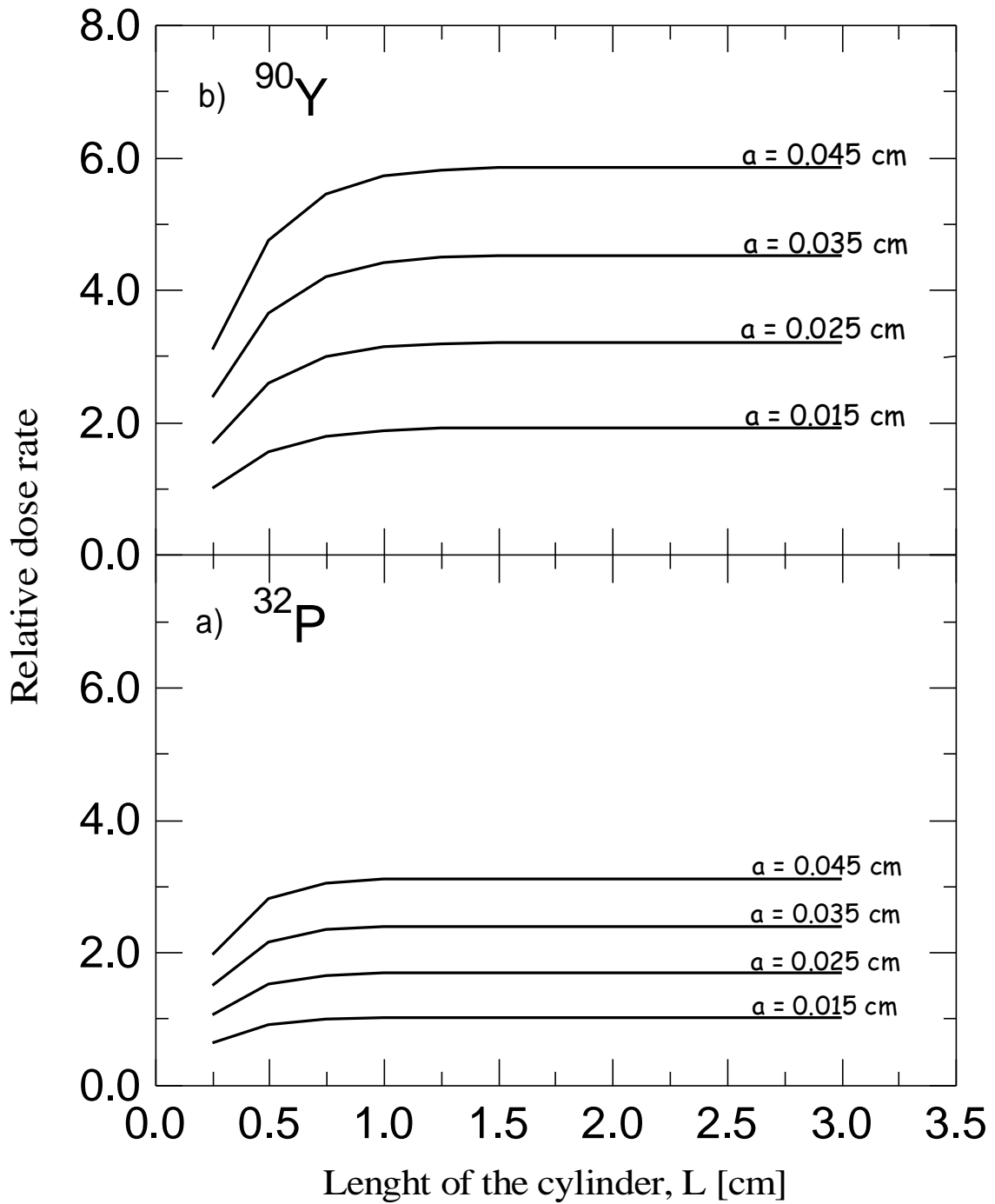


Figure 5. Dose rates relative to the dose rate of the cylindrical source of $L = 2.0$ cm and $a = 0.015$ cm (^{32}P source, part a)), and $L = 0.25$ cm and $a = 0.015$ cm (^{90}Y source, part b)) at the reference point as a function of the length of the source for radii ranging from $a = 0.015$ cm to $a = 0.045$ cm.

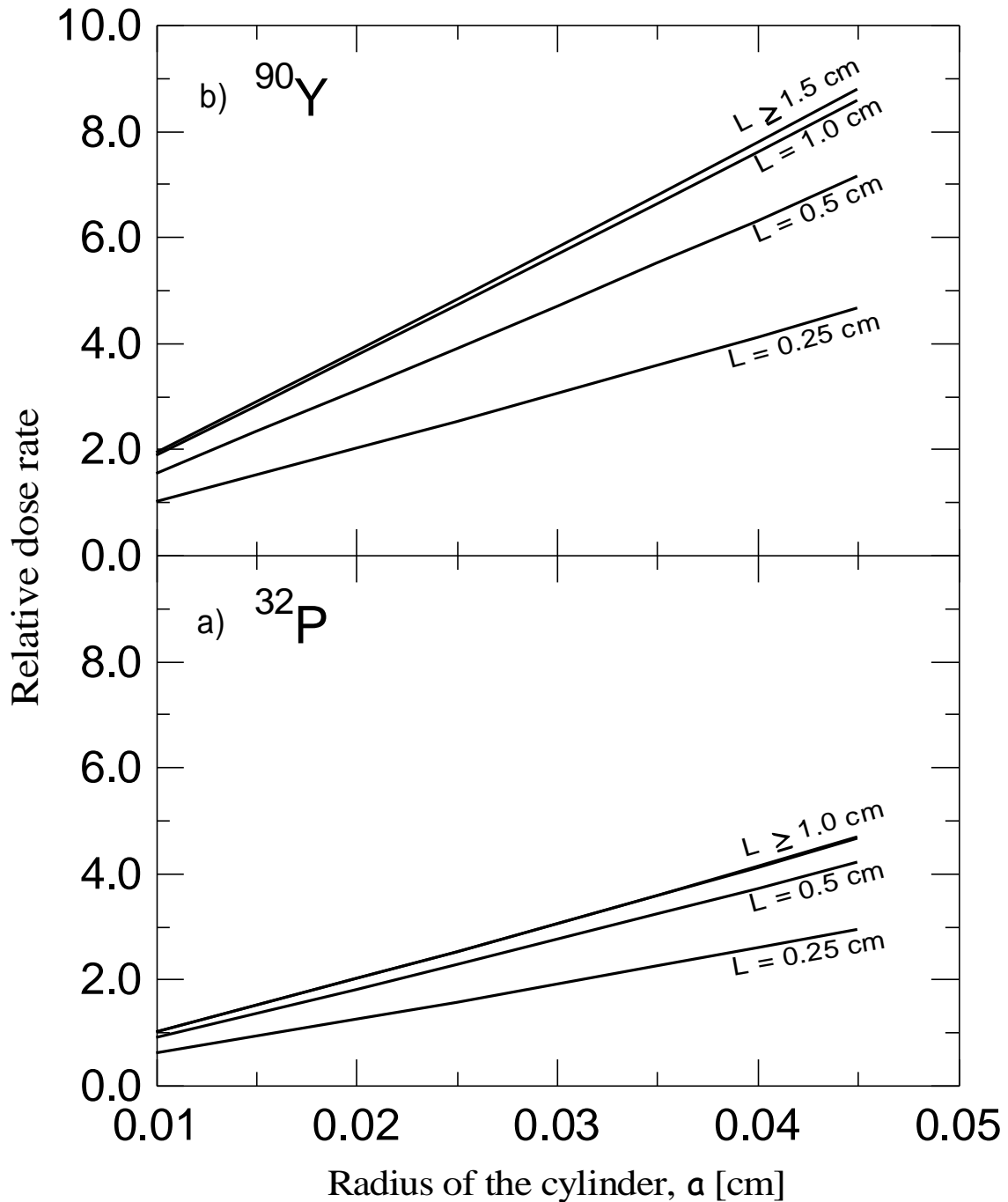


Figure 6. Dose rates relative to the dose rate of the cylindrical source of $L = 2.0$ cm and $a = 0.01$ cm (^{32}P source, part a)), and $L = 0.25$ cm and $a = 0.01$ cm (^{90}Y source, part b)) at the reference point as a function of the radius of the source for lengths ranging from $L = 0.25$ cm to $L = 1.5$ cm.

4. CONCLUSION

In this work a simple numerical routine calculation was developed to estimate the absorbed dose distributions around cylindrical beta sources of ^{32}P and ^{90}Y used in intravascular brachytherapy to prevent the re-closing of arteries. The use of this calculation code to evaluate the absorbed dose rates in water from the cylindrical ^{32}P and ^{90}Y beta sources has allowed to handle with various configurations of radii, lengths and distances in a simple and faster way. The results of the relative dose rates of a such calculations for ^{32}P and ^{90}Y were compared with calculations obtained by published Monte Carlo simulations and in general a good agreement

(differences < 6 %) was found up to radial distances of clinical relevance (~ 0.5 cm) from the center of the cylindrical sources. In spite of the uncertainties associated with the application of this numerical calculation method, it was capable to reproduce successfully the main features of the absorbed dose rates in water around the cylindrical brachytherapy beta sources of ^{32}P and ^{90}Y . However, although the results presented in this work indicate a good agreement with results obtained by Monte Carlo method, a more accurate dose calculation is needed before clinical implementation of the method. Our calculations do not take in consideration the presence of inhomogeneities and the discrepancies increase with distance. Therefore, in the future is proposed to calculate more precisely the absorbed dose distribution for farther distances from the source axis and an inhomogeneity medium surrounding the source be taking into account.

ACKNOWLEDGMENTS

The author would like to thank the referees for their valuable comments and suggestions.

-
1. The International Commission on Radiation Units and Measurements. Dosimetry of beta rays and low-energy photons for brachytherapy with sealed sources. ICRU Report No. 72, 2004.
 2. Stallard HB. Malignant melanoma of the choroid treated with radioactive applicators. *Ann R Coll Surg Engl.* 1961; 29:170–82.
 3. Lommatzch P. Treatment of choroidal melanomas with $^{106}\text{Ru}/^{106}\text{Rh}$ beta-ray applicators. *Surv Ophthalmol.* 1974; 19:85–100.
 4. Char DH, Castro JR. Helium ion therapy for choroidal melanoma. *Arch Ophthalmol.* 1982; 100:935–38.
 5. Packer S, Rotman M, Salanitro P. Iodine-125 irradiation of choroidal melanoma, Clinical experience. *Ophthalmol.* 1984 Dec; 91(12):1700–08.
 6. Augsburger JJ, Gamel JW, Sardi VF, Greenberg RA, Shields JA, Brady LW. Enucleation vs. cobalt plaque radiotherapy for malignant melanomas of the choroid and ciliary body. *Arch Ophthalmol.* 1986;104:655–61.
 7. Char DH, Castro JR, Quivey JM, Phillips TL, Irvine AR, Stone, RD, Kroll S. Uveal melanoma radiation. ^{125}I brachytherapy versus helium ion irradiation. *Ophthalmol.* 1989 Dec; 96(12):1708–15.
 8. Hill C, Sealy R, Shackleton D, Stannard C, Korrubel J, Hering E, Loxton C. Improved iodine-125 plaque design in the treatment of choroidal malignant melanoma. *Br J Ophthalmol.* 1992; 76:91–4.
 9. Jaakkola A, Tommila P, Laatikainen L, Immonen I. Grading choroidal neovascular membrane regression after strontium plaque radiotherapy;masked subjective evaluation vs planimetry. *Eur J Ophthalmol.* 2001; 11:269-76.
 10. Cooper JS. Postoperative irradiation of pterygia: ten more years of experience. *Radiol.* 1978; 128:753-56.
 11. Lommatzsch PK. Results after beta-irradiation ($^{106}\text{Ru}/^{106}\text{Rh}$) of the choroidal melanomas: 20 years experience. *Br J Ophthalmol.* 1996; 70:844-51.
 12. Bice W, Prestidge B, Grimm P, Friedland J, Feygelman V, Roach M, Prete J, Dubois D, Blasko J. Centralized multiinstitutional postimplant analysis for interstitial prostate brachytherapy. *Int J Radiat Oncol Biol Phys.* 1998 Jul;41(4):921-27.
 13. Halligan J, Stelzer K, Rostomily R, Spence A, Griffin T, Berger M. Operation and permanent low activity ^{125}I brachytherapy for recurrent highgrade astrocytomas. *Int J Radiat Oncol Biol Phys.* 1996 Jun;35(3):541-47.
 14. Prestige B, Prete J, Buchholz T, Friedland J, Stock R, Grimm P, Bice W. A survey of current clinical practice of permanent prostate brachytherapy in the United States. *Int J Radiat Oncol Biol Phys.* 1998 Jan;40(2):461-65.
 15. Amols HI. Review of endovascular brachytherapy physics for prevention of restenosis. *Cardiovasc Radiat Med.* 1999;1(1):64-71.

16. Chiu-Tsao S-T, Schaart DR, Soares CG, Nath R. Dose calculation formalisms and consensus dosimetry parameters for intravascular brachytherapy dosimetry: Recommendations of the AAPM Therapy Physics Committee Task Group No. 149. *Med Phys.* 2007 Nov;34(11):4126-57.
17. Mourtada F, Soares CG, Seltzer SM, Lott SH. Dosimetry characterization of ^{32}P source catheter-based vascular brachytherapy source wire. *Med Phys.* 2000 Aug;27(8):1770-76.
18. Chu C-H, Hsieh B-T, Chen I-J, Chen W-L, Lin U-T. Dosimetry study for beta-radiation treatment of in-stent restenosis. *Radiat Prot Dosim.* 2009;134(1):49-54.
19. Massillon-JL G, Minniti R, Mitch MG, Maryanski MJ, Soares CG. The use of gel dosimetry to measure the 3D dose distribution of a $^{90}\text{Sr}/^{90}\text{Y}$ intravascular brachytherapy seed. *Phys Med Biol.* 2009;54(6):1661-72.
20. Karimian A, Saghmanesh S. A dosimetry evaluation of ^{90}Y -stent implantation in intracoronary radiation treatment. *Nucl Tech Radiat Prot.* 2013;28(3):278-83.
21. Rogers DWO. Fifty years of Monte Carlo simulations for medical physics. *Phys Med Biol.* 2006;51:R287-R301.
22. Loevinger R. The dosimetry of the beta sources in tissue. The point source dose function. *Radiol.* 1956;66:55-62.
23. Vynckier S, Wambersie A. Dosimetry of beta sources in radiotherapy I. The beta point source dose function. *Phys Med Biol* 1982;27(11):1339-47.
24. Vynckier S, Wambersie A. Dosimetry of beta sources in radiotherapy: Absorbed dose distributions around plane sources. *Radiat Prot Dosim.* 1986;14(2):169-73.
25. Cross WG. Empirical expressions for beta ray point source dose distributions. *Radiat Prot Dosim.* 1997;69(2):85-96.
26. Mourtada F, Soares CG, Seltzer SM, Bergstrom Jr PM, Fernández-Verea JM, Asenjo J, Lott SH. Dosimetry characterization of a ^{32}P source wire used for intravascular brachytherapy with automated stepping. *Med Phys.* 2003 May;30(5):959-71.
27. Torres J, Buades MJ, Almansa JF, Guerrero R, Lallena AM. Dosimetry characterization of ^{32}P intravascular brachytherapy source wires using Monte Carlo codes PENELOPE and GEANT4. *Med Phys.* 2004 Feb;31(2), 296-304.
28. Saghmanesh S, Karimian A, Abdi M. Absorbed dose assessment of cardiac and other tissues around the cardiovascular system in brachytherapy with $^{90}\text{Sr}/^{90}\text{Y}$ source by Monte Carlo simulation. *Radiat Prot Dosim.* 2011(2);147, 296-99.